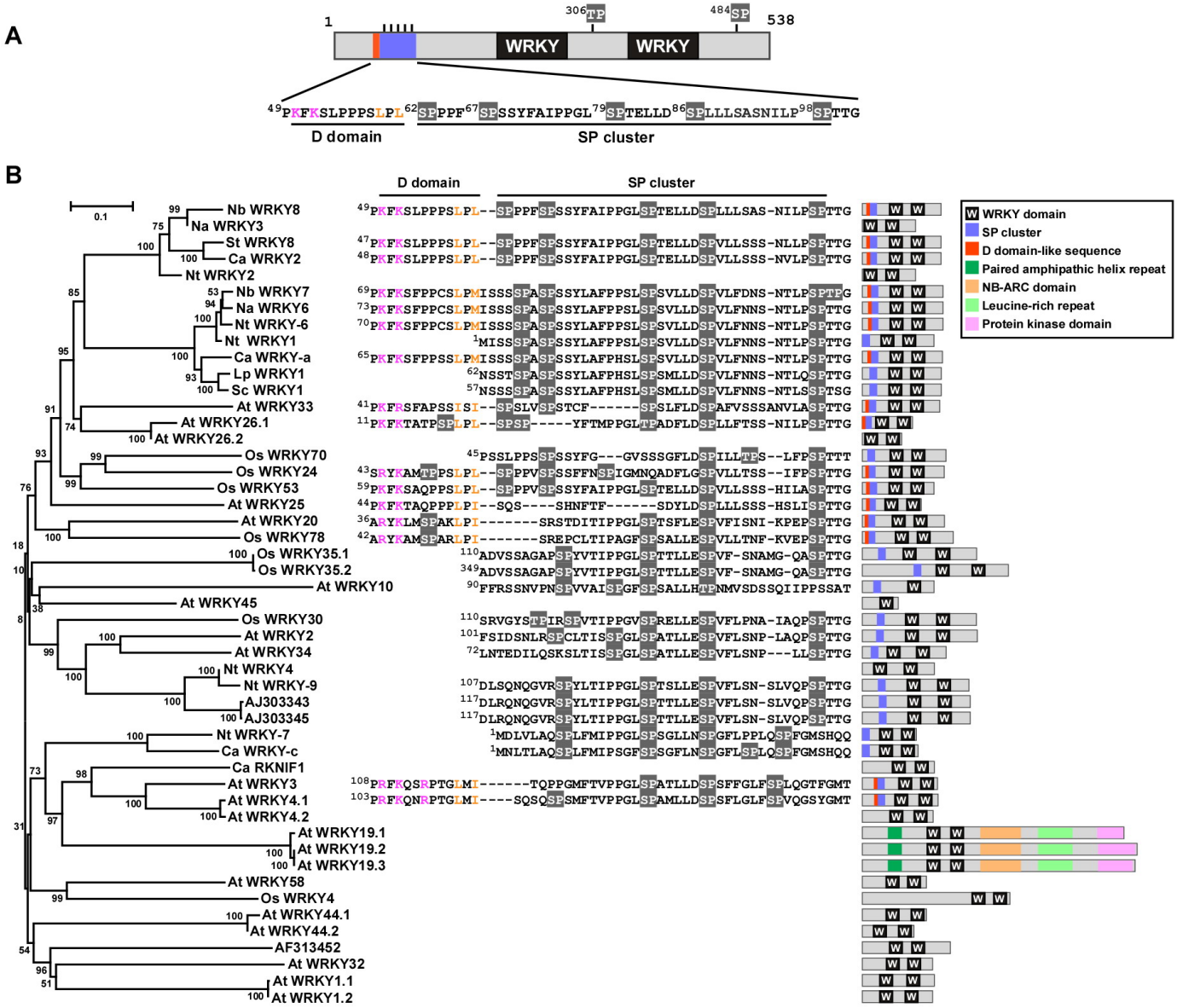

Supplemental Figure 1. SP Cluster and D Domain Widely Conserved in the N-Terminal Region of Group I WRKY Proteins.

(A) Schema of Nb WRKY8 protein showing positions of the D domain, SP cluster and WRKY domain. Lysines and leucines conserved in the D domain were indicated in pink and orange, respectively. Serines or threonine followed by proline (SP or TP) of WRKY8 were highlighted by gray. The numbers indicate position of amino acids of Nb WRKY8 protein.

(B) Left, entire lengths of *Arabidopsis*, rice and solanaceous plant group I WRKY proteins were aligned, and the unrooted tree was constructed by using the neighbor-joining method. Species acronyms are included before the protein name: At, *Arabidopsis thaliana*; Ca, *Capsicum annuum*; Lp, *Lycopersicon peruvianum*; Na, *Nicotiana attenuata*; Nb, *Nicotiana benthamiana*; Nt, *Nicotiana tabacum*; Os, *Oryza sativa*; Sc, *Solanum chacoense*; St, *Solanaum tuberosum*. Middle, amino acid sequences of the SP cluster and D domain adjacent to the N-terminal side of the SP cluster of each WRKY protein. Right, protein structures of each WRKY protein. The bootstrap values for the branches are shown. Accession numbers are shown in Supplemental Table 1 online. The scale bar represents 0.1 amino acid substitutions per site in the primary structure.

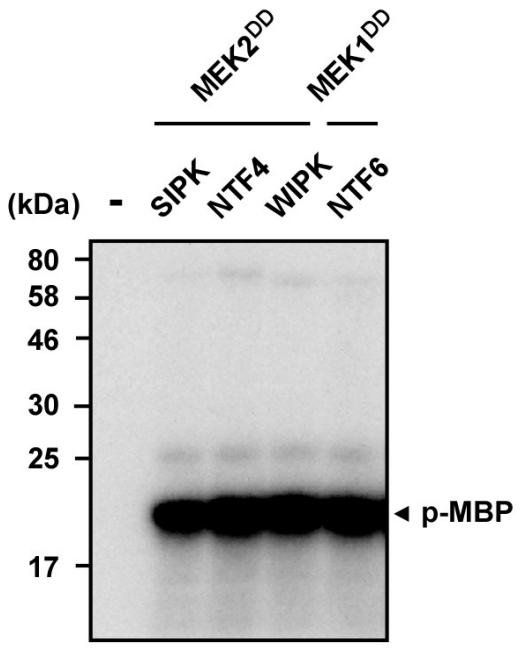

Supplemental Figure 2. In vitro Phosphorylation of MBP by Recombinant MAPKs.

Wild-type GST-tagged MAPKs (SIPK, NTF4, WIPK, and NTF6) were incubated with their corresponding constitutively active MAPKK (i.e., $MEK2^{DD}$ and $MEK1^{DD}$) in the presence of unlabeled ATP. MBP and ^{32}P-labeled ATP were then added. The reaction mixtures were separated using SDS-PAGE and were exposed to X-ray film. Phosphorylated MBPs (p-MBP), which reflect the activity of MAPK, were visualized by autoradiography after SDS-PAGE.

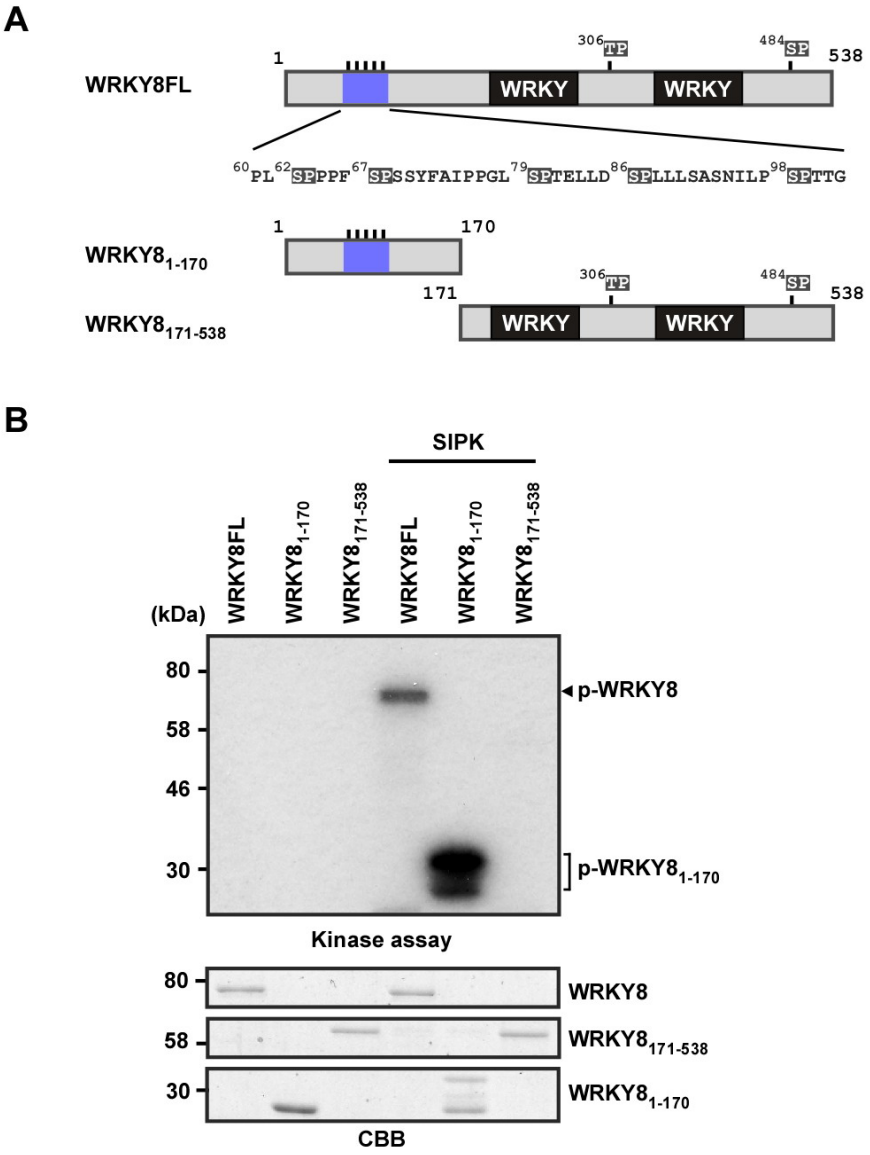

Supplemental Figure 3. The N-terminal Region of WRKY8 Is Phosphorylated by SIPK.

(A) Schematic representation of full-length WRKY8 (WRKY8FL) and truncation constructs $WRKY8_{1-170}$ and $WRKY8_{171-538}$.
(B) In vitro phosphorylation of full-length and truncated WRKY8 by SIPK. Purified Trx-fused WRKY8 variants were used as substrates for active SIPK. Reaction mixtures were separated by SDS-PAGE, stained with CBB (lower panel) and exposed to X-ray film (Kinase assay, upper panel). The position of phosphorylated WRKY8 and $WRKY8_{1-170}$ is shown.

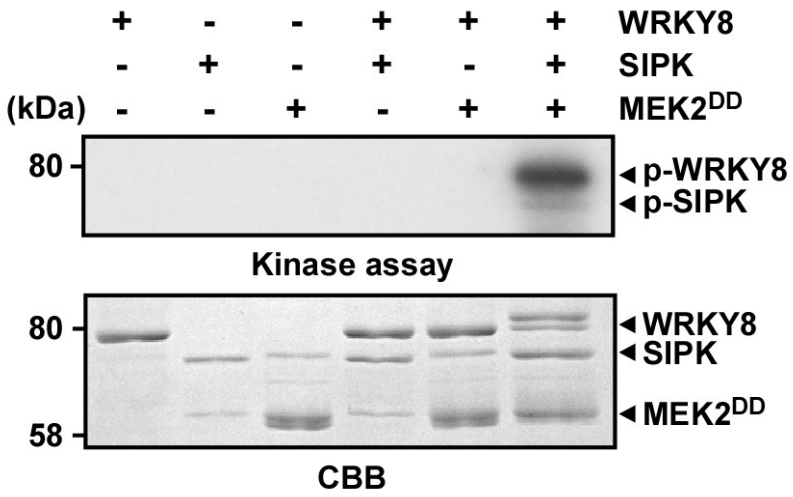

Supplemental Figure 4. In vitro Phosphorylation Analysis of WRKY8 by Recombinant MEK2^{DD}.

In vitro kinase assays were done in the presence of ^{32}P-labeled ATP with the indicated combinations of recombinant proteins. Reaction mixtures were separated by SDS-PAGE, stained with CBB (lower panel) and were exposed to X-ray film (Kinase assay, upper panel). The positions of phosphorylated WRKY8 and SIPK are shown.

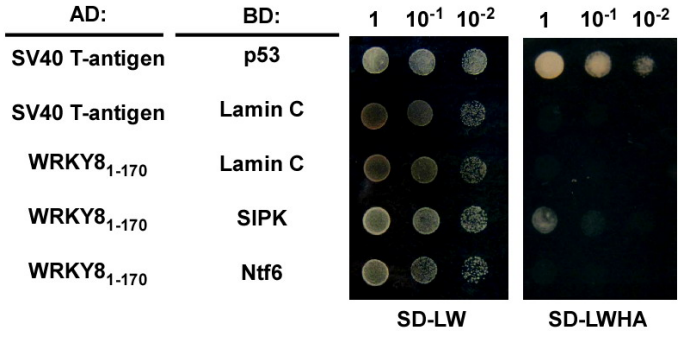

Supplemental Figure 5. Y2H Analysis of the Interaction Between $WRKY8_{1-170}$ and SIPK.

Yeast was co-transformed with the constructs indicated, carrying a binding domain (BD) and an activation domain (AD), and was grown on SD media lacking Leu and Trp (SD-LW) or Leu, Trp, His, and adenine (SD-LWHA). SV40 T-antigen with p53 protein or with Lamin C were used as positive and negative controls, respectively.

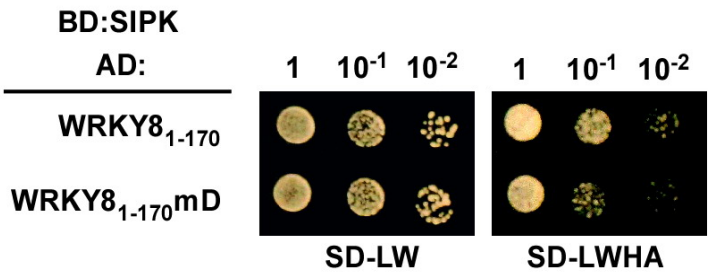

Supplemental Figure 6. Y2H Analysis of the Interaction Between $WRKY8_{1-170}$mD and SIPK.

Yeast was co-transformed with the constructs indicated, carrying a binding domain (BD) and an activation domain (AD), and was grown on SD-LW medium or SD-LWHA medium.

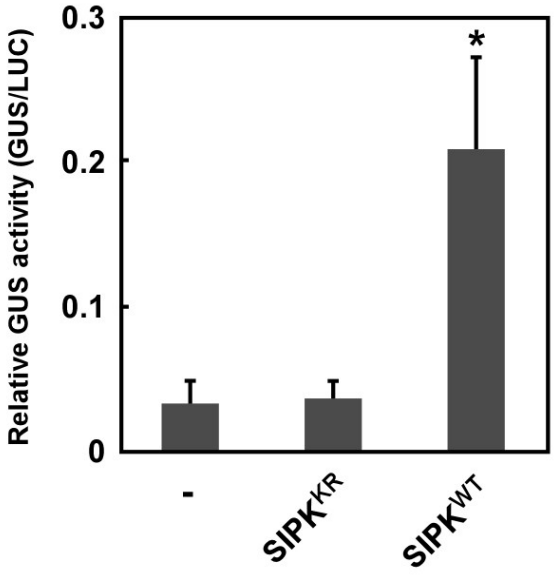

Supplemental Figure 7. Increased Transactivation Activity of GAL4DBD-WRKY8$^{WT}_{1-170}$ by SIPK-Mediated Phosphorylation.

Agrobacterium strains contained GAL4-WRKY8$^{WT}_{1-170}$, SIPK variants, reporter plasmids and reference plasmids at ratio 1:1:2:1 (final OD_{600} 0.25). For reporter plasmids, six tandem repeats of the GAL4 upstream activation sequence (CGGAGTACTGTCCTCC G) were fused upstream of the minimal 35S promoter (-46) and Ω sequence, and were cloned into pGreen. The cDNA of the *GUS* reporter gene containing one intron was subsequently cloned behind the synthetic promoter. At 48 h after agroinfiltration, total proteins were extracted from leaf tissues. Data are means ± SDs from three independent experiments. **P* < 0.01 versus the GAL4DBD-WRKY8$^{WT}_{1-170}$ alone by two-tailed student's *t* test.

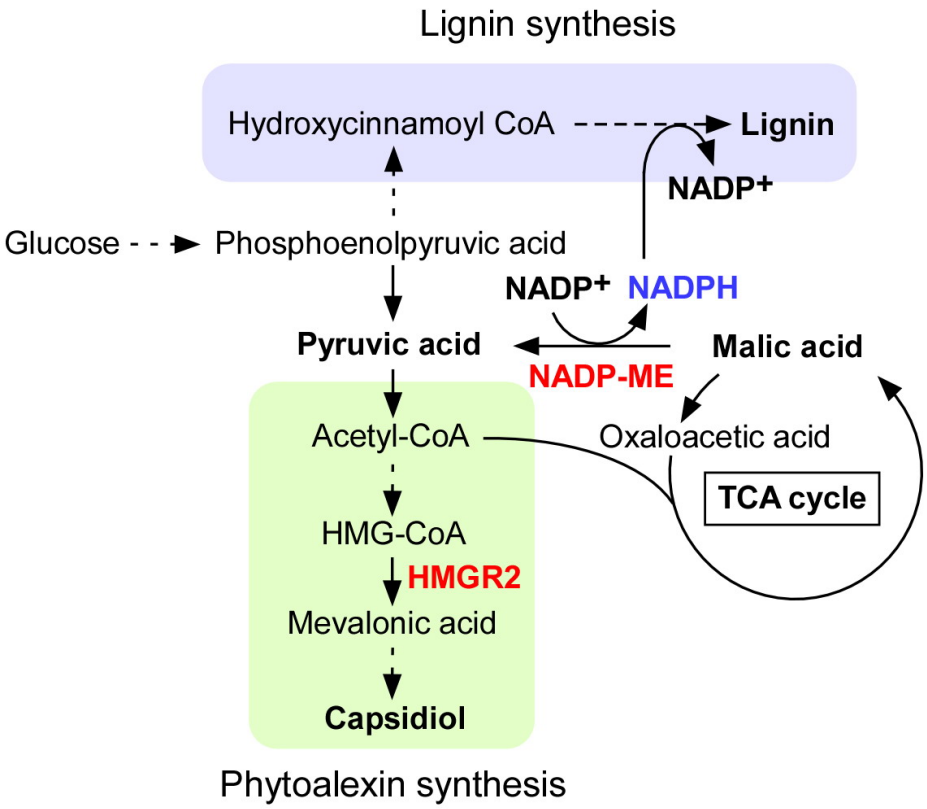

Supplemental Figure 8. Schematic Representation of Defense-Related Metabolic Pathways Induced by WRKY8.

HMGR catalyzes the rate-limiting step in biosynthesis of the sesquiterpenoid compound capsidiol, a major tobacco anti-fungal phytoalexin. NADP-ME catalyzes oxidative decarboxylation of malic acid, producing pyruvate, CO_2, and NADPH, and is suggested to participate in the plant defense response by providing NADPH for lignification of the cell wall (Wheeler et al., 2005).

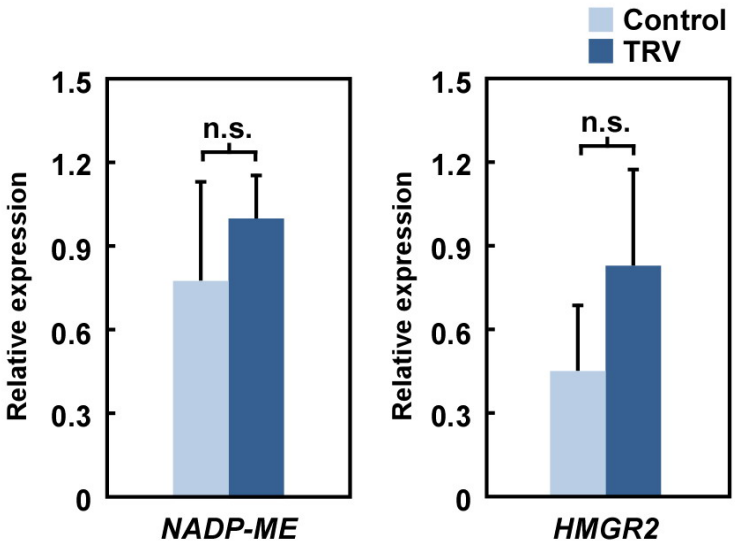

Supplemental Figure 9. Expression Analysis of *NADP-ME* and *HMGR2* in *N. benthamiana* in Response to TRV Infection.

Total RNA was isolated from TRV-infected (TRV) or uninfected (Control) leaves of *N. benthamiana* with no treatment and were used for qRT-PCR. Data are means ± SDs from four independent experiments. n.s. = not significant ($P > 0.05$, two-tailed student's *t* test).

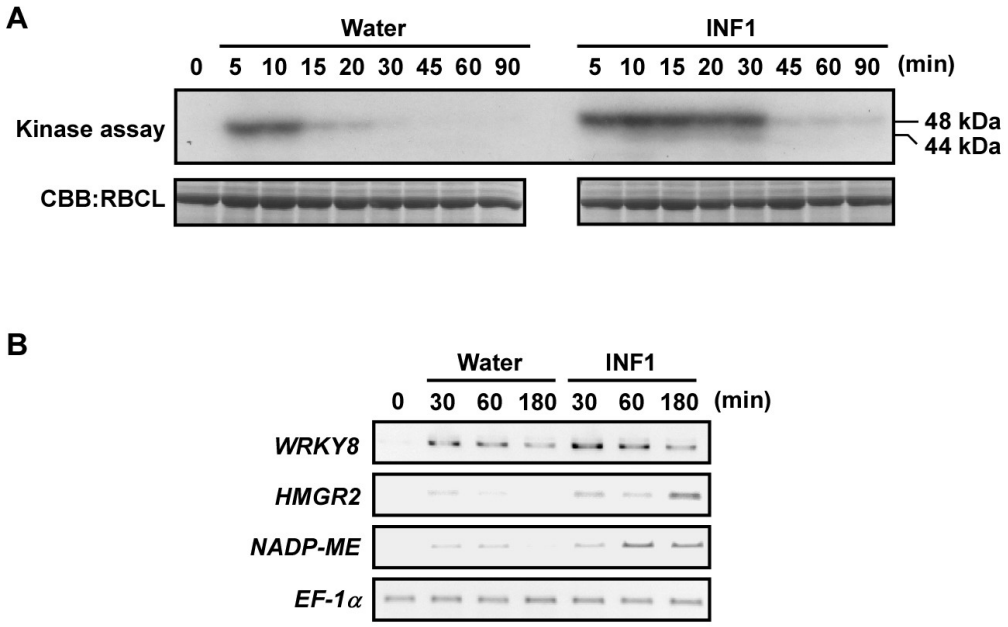

Supplemental Figure 10. Activation of MBP Kinase Activity and Expression of Downstream Genes of WRKY8 Induced by INF1 Treatment.

(A) *N. benthamiana* leaves were infiltrated with either 10 μg/mL INF1 or water, and samples were taken at the indicated times. Kinase activity was determined by in-gel kinase assay using MBP as a substrate. The molecular masses of the activated kinases are given in kilodaltons (kDa).
(B) Gene expression profiles were monitored by using RT-PCR. Samples were taken at the indicated times as similar to **(A)**. The experiment was repeated three times and typical data was shown.

Supplemental Table 1.

Accession numbers of the amino acid sequences included in the phylogenic tree.
AJ303343.1, CAC36397.1; AJ303345.1, CAC36402.1; AtWRKY1.1, NP_178565.1; AtWRKY1.2, NP_849936.1; AtWRKY2, NP_200438.1; AtWRKY3, NP_178433.1; AtWRKY4.1, NP_172849.1;AtWRKY4.2, NP_849658.1; AtWRKY10, NP_175956.1; AtWRKY19.1, NP_192939.2; AtWRKY19.2, NP_001118968.1; AtWRKY19.3, NP_001154222.1; AtWRKY20, NP_849450.1; AtWRKY25, NP_180584.1; AtWRKY26.1, NP_196327.1; AtWRKY26.2, NP_974746.1; AtWRKY32, NP_567862.3; AtWRKY33, NP_181381.2; AtWRKY34, NP_194374.1; AtWRKY44.1, NP_181263.2; AtWRKY44.2, NP_001078015.1; AtWRKY45, NP_186846.1; AtWRKY58, NP_186757.2; CaRKNIF1, ABA56495.2; CaWRKY2, ABD65255.1; CaWRKY-a, AAR26657.1; CaWRKY-c, AAW67002.1; LpWRKY1, ABI95141.1; NaWRKY3, AAS13439.1; NaWRKY6, AAS13440.1; NbWRKY7, BAI63295.1; NbWRKY8, BAI63296.1; NtWRKY1, BAA82107.1; NtWRKY2, BAA77383.1; NtWRKY4, BAA86031.1; NtWRKY-6, BAB61053.1; NtWRKY-7, BAB61054.1; NtWRKY-9, BAB61056.1; OsWRKY4, NP_001051337.1; OsWRKY24, NP_001044675.1; OsWRKY30, NP_001062148.1; OsWRKY35.1, AAQ20910; OsWRKY35.2, NP_001053057.1; OsWRKY53, NP_001055252.1; OsWRKY70, NP_001055828.1; OsWRKY78, NP_001060116.1; ScWRKY1, AAQ72790.1; StWRKY8, BAI63294.1.